

Large mode area and nearly zero flattened dispersion photonic crystal fiber by diminishing the pitch of the innermost air-holes-ring

Jiajia zhao (赵佳佳)¹, Jin Hou (侯金)^{1*}, Chunyong Yang (杨春勇)¹,
Zhiyou Zhong (钟志有)¹, Yihua Gao (高义华)², and Shaoping Chen (陈少平)¹

¹Hubei Key Laboratory of Intelligent Wireless Communications, College of Electronics
and Information Engineering, South-central University for Nationalities,
Wuhan 430074, China

²Wuhan National Laboratory for Optoelectronics (WNLO), School of Physics, Huazhong
University of Science and Technology, Wuhan 430074, China

*Corresponding author: houjin@mail.scuec.edu.cn

Received October 5, 2013; accepted October 16, 2013; posted online March 3, 2014

In this study, we propose that by diminishing only the pitch of the innermost air-holes-ring of a HF1 photonic crystal fiber, both an effective mode area up to $100 \mu\text{m}^2$ at $1.55 \mu\text{m}$ wavelength and nearly zero dispersion of $0.2 \pm 1 \text{ ps}/(\text{km} \cdot \text{nm})$ within a spectrum range of $1.23\text{--}1.65 \mu\text{m}$ can be achieved simultaneously. Because only one parameter is needed to be tuned in the proposed design scheme, the fiber would be easier to be fabricated compared to other fibers using either multiple changing parameters or additional kinds of materials and would have potential applications in optical communications.

OCIS codes: 060.5295, 060.2270, 060.2430, 060.2280.

doi: 10.3788/COL201412.S10607.

Photonic crystal fiber (PCF) has attracted great research attentions because of its unique optical properties and flexible designs since it was firstly fabricated in 1996^[1]. It is also being considered to have the potential to be a pre-eminent method for information transmission in wavelength-division multiplexing (WDM) system. However, with the requirement of large information capacity and long transmission distance in WDM system, the problem of nonlinear effects and dispersion became an obstacle to the PCFs' wide application. A possible solution to this issue is to design large mode area and nearly zero dispersion flattened PCFs. Over the last decade, various techniques such as using different air-holes diameters for different rings^[2-4], replacing circle air-holes by elliptical air-holes^[5,6], doping GeO_2 in the central part of the silica core^[7,8], and filling the air-holes with index matching liquids^[9] have been employed to flatten the dispersion curves of PCFs. But their corresponding effective mode areas are not considered. In 2006, a PCF with both large mode area and flattened dispersion was obtained by using an artificially defected air-hole ring in the cladding and also assembling additional defected air-holes in the central core region of the fiber^[10]. Recently, through insertion of a square configuration defect in the core of a HF7 PCF^[11], a first fully systematic procedure to design a large mode area, dispersion flattened single-mode PCF was presented^[12]. However, in these types of PCFs, multiple design parameters are adopted, which would not only raise the complexity of the fibers' design but also increase the difficulty of the fibers' fabrication. Therefore, a simple design scheme to realize PCFs with both large mode area and ultra-flattened dispersion would have great significance.

In this letter, we presented a PCF with both large effective mode area and nearly zero flattened dispersion

by only diminishing the innermost air-holes-ring's pitch. Numerical results show that, in an optimized PCF, both a flattened chromatic dispersion of $0.2 \pm 1 \text{ ps}/(\text{km} \cdot \text{nm})$ within a wavelength range from 1.23 to $1.65 \mu\text{m}$ and an effective mode area more than $100 \mu\text{m}^2$ at $1.55 \mu\text{m}$ wavelength can be achieved.

Our design is based on a previous investigated PCF^[12], which obtained a large effective mode area while maintained a flattened dispersion by precisely adjusting the diameter and position of the defect air-holes in a HF7 PCF. In our design, we expect that by only diminishing the pitch of innermost air-holes-ring in a HF1 PCF^[11], a similar performance would be obtained with a relative simpler structure. Figure 1 shows the schematic cross-section of the proposed PCF. It is composed of circular air-holes arranged in a hexagonal lattice in the background of pure silica. The silica core is formed by removal of a single air-hole in the fiber centre and the number of the air-hole-rings is assumed to be 11, which is also well known as HF1 PCF. The diameter of air-holes d is assumed to be $0.8 \mu\text{m}$, and the lattice constant Λ is with $2.5 \mu\text{m}$. Here, considering the state of the art in the fiber fabrication, the value of Λd should not be too small. So the scope of parameter Λd is limited from $2.5 \mu\text{m}$ to $1.0 \mu\text{m}$.

The chromatic dispersion $D(\lambda)$ of a PCF contains waveguide dispersion and material dispersion, which can be calculated from the second derivation of the real part of the effective mode index as^[13]

$$D(\lambda) = -\frac{\lambda}{c} \frac{d^2 \text{Re}(n_{\text{eff}})}{d\lambda^2}, \quad (1)$$

where c is the speed of light in vacuum, the effective index n_{eff} of the fundamental mode in PCF is obtained by solving the Maxwell equations as an eigenvalue problem

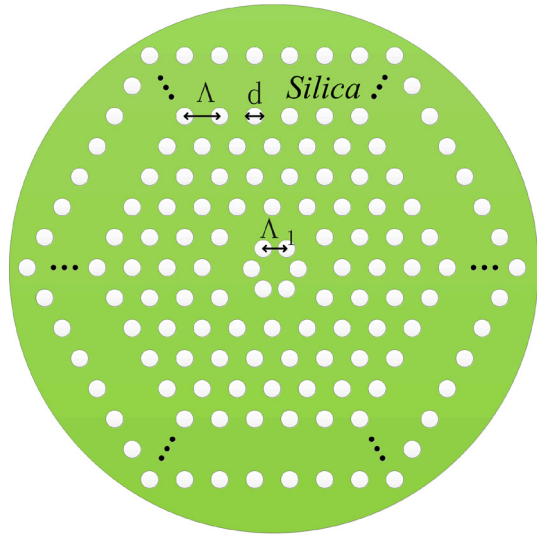


Fig. 1. Schematic cross section of the proposed 11 ring PCF. The air-holes in the silica cladding region are arranged in a hexagonal configuration with lattice constant Λ and air-holes diameter d . The air-holes pitch of the innermost ring is reduced to Λ_1 .

with a plane-wave expansion method^[14]. The effective area of the fundamental mode A_{eff} is using the following definition^[15]:

$$A_{eff} = \frac{\left(\iint_S |E_t|^2 dx dy \right)^2}{\iint_S |E_t|^4 dx dy}, \quad (2)$$

where E_t is the transverse electric field vector and S denotes the whole fiber cross-section.

Fig. 2 shows the calculated chromatic dispersion curves as a function of the wavelength λ with $d = 0.8 \mu\text{m}$ and $\Lambda = 2.5 \mu\text{m}$, for a changing Λ_1 within a range from 2.5 to 1.0 μm . The black solid curve represents the chromatic dispersion of the initial fiber with $\Lambda_1 = \Lambda = 2.5 \mu\text{m}$. The blue solid curves with various geometric shapes show that the chromatic dispersion curves shift down with the decreasing of Λ_1 from 2.4 μm to 2.1 μm in a step of 0.1 μm . The red dash-dot curves with various geometric shapes describe the chromatic dispersion shift upward with a further decreasing of Λ_1 from 2.0 μm to 1.0 μm in a step of 0.2 μm .

Comparing the blue solid curves with the red dash-dot curves, we find that a slight decrement of Λ_1 from its initial value gains a greater impact to the variation of dispersion than further decrement of Λ_1 . The dispersion curve firstly shifts downward as the decrement of Λ_1 . While the dispersion curve is decreasing downward, the point of the greatest decline in the dispersion curve is gradually moving from longer wavelength zone to shorter wavelength zone. However, when the decrement of Λ_1 is beyond a specific critic value, the dispersion curve turns to shift upward. While the dispersion curve is shifting upward, the point of the greatest decline is moving from shorter wavelength zone to longer wavelength zone. Therefore, there must be an optimum Λ_1 value for the proposed PCF, at which a flattened

dispersion curve around the wavelength of communication band would be obtained. From the result shown in Fig. 2, the optimum dispersion curve is with $\Lambda_1 = 1.8 \mu\text{m}$, and its dispersion variation is only $0.2 \pm 1 \text{ ps}/(\text{km} \cdot \text{nm})$ within in a wavelength range of 1.23 ~ 1.65 μm .

Moreover, the effective mode area variation with the changing of Λ_1 is also given in Fig. 3. As shown in Fig. 3(a), when $\Lambda_1 = \Lambda = 2.5 \mu\text{m}$, the fundamental mode electric field distributions is limited to the innermost ring, and the effective mode area at the wavelength of 1.55 μm is less than 20 μm^2 . On the other side, as shown in Fig. 3(b), when Λ_1 is decreased to its optimum with 1.8 μm , the effective mode area soars greatly to 102 μm^2 at the same wavelength. As Λ_1 decreased, mode field tends to distribute mainly in the space between the innermost and the neighborhood air-holes-ring. Obviously, the area covered by the mode field in Fig. 3(b) is far larger than that in Fig. 3(a). Having understood the influence of the innermost air-holes pitch on the chromatic dispersion and effective mode area of PCF, we also can use the method to tailor the effective mode area and chromatic dispersion of PCF for other applications.

In conclusion, we investigate and analyze the influence exerted by the pitch of the innermost air-holes-ring on the chromatic dispersion and effective mode area in a PCF. According to the method mentioned above, a PCF both with large effective mode area beyond 100 μm^2 at 1.55 μm wavelength and ultra-flattened dispersion of $0.2 \pm 1 \text{ ps}/(\text{km} \cdot \text{nm})$ in a wavelength range of 1.23–1.65 μm is achieved. The proposed PCF reduces the difficulty of fabrication compared to other design schemes using either multiple changing parameters or additional kinds of materials. The design principle presented here can also be applicable for square lattice PCFs. Taking all these things into account, the

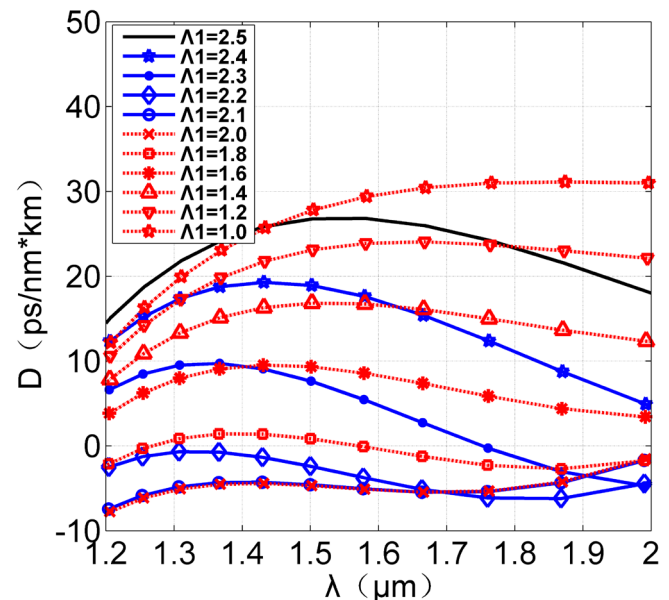


Fig. 2. Chromatic dispersion curves as a function of the wavelength λ for different Λ_1 values, with $d = 0.8 \mu\text{m}$ and $\Lambda = 2.5 \mu\text{m}$.

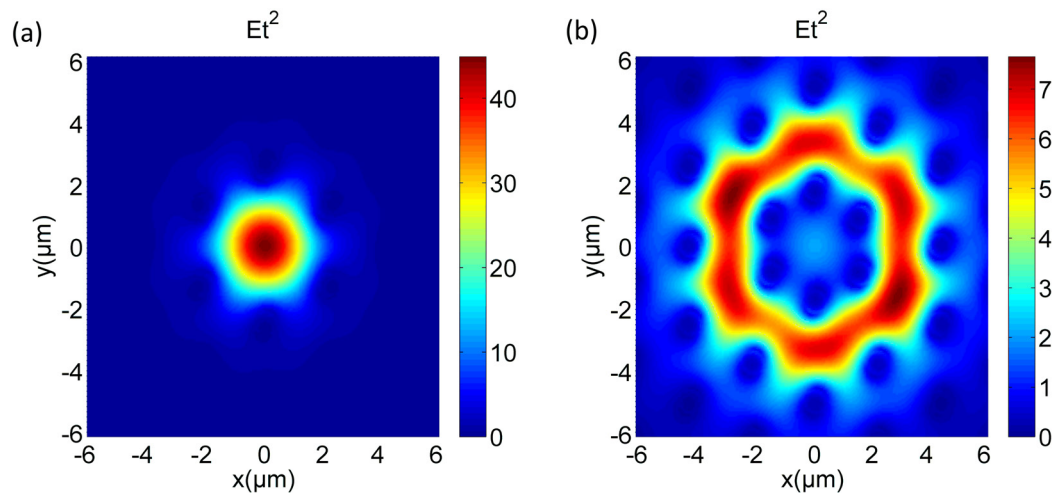


Fig. 3. Fundamental mode electric field intensity distributions for PCFs with different innermost pitch sizes. (a) $\Lambda_1 = 2.5 \mu\text{m}$, (b) $\Lambda_1 = 1.8 \mu\text{m}$.

proposed PCF would have a wide application in ultra-broadband WDM transmission system.

This work was supported partly by National Natural Science Foundation of China under Grant Nos. 11147014, 61002013 and 11074082, the Natural Science Foundation of Hubei Province under Grant No. 2013CFA052, and also partly by the open fund of Hubei Key Laboratory of Intelligent Wireless Communications under Grant No. IWC2012009.

References

1. J. C. Knight, T. A. Birks, P. St. J. Russell, and D. M. Atkin, *Opt. Lett.* **21**, 1547 (1996).
2. H. Xu, J. Wu, Y. Dai, C. Xu, and J. Lin, *Chin. Opt. Lett.* **9**, 050603 (2011).
3. T. L. Wu and C. H. Chao, *IEEE Photon. Technol. Lett.* **17**, 67 (2005).
4. Y. Li, B. Liu, Z. Wang, M. Hu, and Q. Wang, *Chin. Opt. Lett.* **2**, 75 (2004).
5. N. H. Hai, Y. Namihira, S. Kaijage, F. Begum, S. M. A. Razzak, T. Kinjo, and N. Zou, in *proceedings of IEEE CLEO/Pacific Rim 2007*, 1 (2007).
6. N. H. Hai, Y. Namihira, S. F. Kaijage, T. Kinjo, F. Begum, S. M. A. Razzak, and N. Zou, *Opt. Rev.* **15**, 91 (2008).
7. Y. Hoo, W. Jin, J. Ju, H. Ho, and D. Wang, *Opt. Commun.* **242**, 327 (2004).
8. S. Lou, H. Fang, H. Li, T. Guo, L. Yao, L. Wang, W. Chen, and S. Jian, *Chin. Opt. Lett.* **6**, 821 (2008).
9. K. M. Gundu, M. Kolesik, J. V. Moloney, and K. S. Lee, *Opt. Express* **14**, 6870 (2006).
10. N. Florous, K. Saitoh, and M. Koshiba, *Opt. Lett.* **14**, 901 (2006).
11. K. Saitoh, Y. Tsuchida, M. Koshiba, and N. A. Mortensen, *Opt. Express* **13**, 10833 (2005).
12. A. Rostami and H. Soofi, *J. Lightwave Technol.* **29**, 234 (2011).
13. A. Ferrando, E. Silvestre, J. J. Miret, and P. Andres, *Opt. Lett.* **25**, 790 (2000).
14. Z. Wang, S. Lou, and S. Jian, *Opt. Express* **11**, 980 (2003).
15. M. Koshiba and K. Saitoh, *Opt. Express* **11**, 1746 (2003).